Zirconium Nano Building Blocks Based on the 3-Butynoic Acid Ligand: Synthesis and Thermomechanical Studies of the Resulting Inorganic–Organic Hybrid Material

Simona Maggini, Fabrizio Girardi, Klaus Müller, Rosa Di Maggio

Dipartimento di Ingegneria dei Materiali e Tecnologie Industriali, Università degli Studi di Trento, Trento, Italy

Received 18 May 2011; accepted 8 July 2011
DOI 10.1002/app.35217
Published online 26 October 2011 in Wiley Online Library (wileyonlinelibrary.com).

ABSTRACT: A new zirconium nano building block (ZrNBB) was prepared by the reaction of Zirconium tetrapropoxide with 3-butynoic acid in an alkoxide/acid at a 1 : 3 or 1 : 6 molar ratio. The complex was characterized by FTIR, ^{1}H-NMR and ^{13}C-NMR spectroscopy, thermogravimetric analysis, differential scanning calorimetry, energy-dispersive X-ray analysis, and elementary analysis. A spontaneous alkyne-to-allene isomerization process was observed for ZrNBB. A bulk sample was also prepared and analyzed via dynamical mechanical spectroscopy in compression mode. The zirconium complex was then embedded in a polymeric matrix by radical copolymerization with vinyl trimethoxysilane. The inorganic–organic hybrid material was chemically and thermally stable. The shear storage modulus and loss modulus were measured to determine the mechanical properties of the material. The preliminary results are presented. © 2011 Wiley Periodicals, Inc. J Appl Polym Sci 124: 2110–2117, 2012

Key words: copolymers; flame retardance; glass transition; mechanical properties; transition metal chemistry

INTRODUCTION

Hybrid materials synthesized from organically modified transition-metal oxide clusters often retain the well-defined structure and original properties of the clusters.[1] This allows for better control of the size and dispersion of the inorganic component and the use of rational design principles to obtain materials with enhanced properties.[2] In our group, reinforced inorganic–organic hybrid polymers composed from the zirconium nano building block {ZrNBB; $[Zr_6O_4(OH)_4$(vinyl acetoxylate$)_{12}$(*n*-PrOH)$]_2 \cdot 4$(vinyl acetic acid)} and vinyl trimethoxysilane (VTMS) were developed and have proven to have excellent thermomechanical performance with applications as coatings for wood and paper protection.[3] In this work, with the aim of obtaining better control of the structure and assembly route of the coating, we varied the interface between the inorganic and organic components via modification of the ZrNBB. The synthesis of a new ZrNBB, where the zirconium was bound to the organic ligand 3-butynoic acid, instead of vinyl acetic acid, is reported here, together with the preparation and the thermomechanical study of the correspondent VTMS copolymer. The 3-butynoic acid was chosen as the organic ligand for its rigidity and its different conformational geometry (i.e., the presence of the triple instead of the double bond). Moreover, the triple bond of the organic ligand can allow, in future studies, the direct introduction of other functional groups through electrophilic or nucleophilic addition to selectively modify the ZrNBB, which would leave a double bond to be employed for polymerization.

In the literature, there are only two examples of metal clusters containing acetylenic carboxylate ligands, $Ti_6O_4(OPr)_8[OOC(CH_2)_2C{\equiv}CH]_8$ and $\{Zr_6O_4(OH)_4[OOC(CH_2)_3C{\equiv}CH]_{12}\}_2 \cdot 6[HOOC(CH_2)_3C{\equiv}CH]$, which were, in principle, introduced for the preparation of cluster-based inorganic–organic hybrid materials through the use of click chemistry.[4]

EXPERIMENTAL

Materials

All commercial reagents and solvents employed were of high-grade purity and were used as supplied without further purification. The anhydrous solvents *n*-propanol 99.7% and tetrahydrofuran (THF) $\geq$99.9% were purchased from Sigma-Aldrich, Steinheim Germany. All manipulations were performed under aerobic conditions unless standard Schlenk techniques were required.

Synthesis of 3-butynoic acid

3-Butyn-1-ol (79.3 mmol) was added slowly to a mixture of $K_2Cr_2O_7$ (0.802 mmol), $NaIO_4$ (174.3

Professor Klaus Müller passed away during the writing of this article. He was a brilliant scientist, a respected colleague, and a good person. This article is dedicated to him.

Correspondence to: S. Maggini (simona.maggini@ing.unitn.it).

Contract grant sponsors: Nanostructured metal oxide and inorganic-organic hybrid coatings for cellulose and lignin (paper and wood) for preservation against fungi and chemical attack and as flame retardant (keywords: Cellulose, Nanocomposites, Coating, Lignin; acronim: CE-NA-CO-LI) of the Provincia Autonoma di Trento.

mmol), and 65% HNO_3 (0.388 g) in H_2O (140 mL). The resulting slurry was stirred at 18–20°C for 24 h and filtered, and the filtrate was extracted with ethyl acetate. The organic phases were combined and dried over Na_2SO_4. The solvent was evaporated, and the desired product was recovered as a white solid (4.64 g, 70%).

Fourier transform infrared (FTIR) spectroscopy (cm^{-1}): 3296 (≡C—H); 3281 (≡C—H); 3200–2900 (O—H); 2946 (CH_2); 2912 (CH_2); 2127 (C≡C); 1688 (C=O); 1423, 1390, 1320, 1287, 1227. ^{13}C-Magic Angle Spinning Nuclear Magnetic Resonance (MAS NMR) spectroscopy (ppm): 174.01 (CO_2), 76.19 (C≡CH), 73.34 (C≡CH), 26.47 (CH_2). ^{1}H-NMR [dimethyl sulfoxide (DMSO), 400 MHz, ppm]: 2.99 (t, 1H, $^4J_{H-H} = 2.6$ Hz, ≡CH), 3.30 (br, 2H, CH_2).

Preparation of ZrNBB

3-Butynoic acid and Zirconium tetrapropoxide {$Zr(OPr^n)_4$] 70% solution in *n*-propanol were mixed at a molar ratio of 6 : 1 or 3 : 1 under an inert atmosphere. The mixture was stirred vigorously at room temperature for 1 h and then washed with anhydrous *n*-propanol. The precipitate was separated by filtration and dried *in vacuo*.

A bulk sample was produced by the mixture of 3-butynoic acid and 70% $Zr(OPr^n)_4$ in *n*-propanol (molar ratio = 3 : 1) at room temperature for 24 h. The solution was evaporated to dryness to leave an orange xerogel. A cylindrical sample with a length of 5.37 mm and a diameter of 4.75 mm was obtained.

Preparation of the ZrNBB–VTMS copolymer in THF

VTMS was added to a solution of ZrNBB in anhydrous THF (Si/Zr molar ratio = 40 : 1); then, benzoyl peroxide (BPO; 1 wt % with respect to VTMS) was added, and the mixture was stirred at room temperature for 1 h. The solution was evaporated to dryness to leave a yellow transparent xerogel (ZrNBB/VTMS/BPO). A cylindrical sample with a length of 1.71 mm and a diameter of 5.97 mm was produced. Dynamic mechanical spectroscopy (DMS) analysis results were as follows: after the first run, 1.64 × 5.93 mm^2, and after the second run, 1.60 × 5.90 mm^2.

Preparation of the ZrNBB–VTMS copolymer in dimethylformamide (DMF)

VTMS was added to a solution of ZrNBB in DMF (Si/Zr molar ratio = 40 : 1); then, BPO (1 wt % with respect to VTMS) was added, and the mixture was stirred at room temperature for 1 h. The solution was evaporated to dryness to leave an orange transparent xerogel (ZrNBB/VTMS/BPO). A cylindrical sample with a length of 3.80 mm and a diameter of 6.10 mm was produced. The DMS analysis results were as follows: after the first run, 3.59 × 5.90 mm^2, and after the second run, 3.57 × 5.89 mm^2.

Preparation of the ZrNBB–VTMS copolymer without a radical initiator

VTMS was added to a solution of ZrNBB in anhydrous THF (Si/Zr molar ratio = 40 : 1), and the mixture was stirred at room temperature for 1 h. The solution was evaporated to dryness to leave a yellow transparent xerogel (ZrNBB/VTMS). A cylindrical sample with a length of 2.86 mm and a diameter of 5.96 mm was produced. The DMS analysis results were as follows: after the first run, 2.65 × 5.36 $mm^{2,}$ and after the 2nd run, 2.43 × 5.63 mm^2.

Instrumentation

Differential scanning calorimetry (DSC) analyses were performed with a DSC92 SETARAM (Setaram, Milano Italy) from 30 to 200°C in nitrogen with a heating rate of 10°C/min. Thermogravimetric analysis was performed from 30 to 1000°C in argon with a heating rate of 10°C/min with a Labsys SETARAM thermobalance. FTIR spectra were recorded in reflectance mode (attenuated total reflection system with a zinc selenide crystal) in the range 4000–400 cm^{-1} with a PerkinElmer Spectrum One instrument. Solid-state NMR analyses were carried out with a Bruker AVANCE 400 WB instrument for ^{1}H (400.13 MHz), ^{29}Si (79.50 MHz), and ^{13}C (100.07 MHz) experiments. The chemical shifts are reported in parts per million (ppm). Samples were packed in 4-mm zirconia rotors, which were spun at 9.5 kHz under air flow. Environmental Scanning Electron Microscope (ESEM) scans were obtained with a Philips ESEM-TMP XL30, and the microanalysis was conducted with a Falcon-EDAX with a carbon–uranium detector connected to the microscope. DMS was performed in compression and shear modes with a Seiko DMS6100 instrument at a frequency of 1 Hz with a linear displacement of 0.005 mm and initial applied forces of 100 and 1000 mN, respectively. The storage modulus (G'), loss modulus (G''), and tan δ were measured in the temperature range 30–300°C with a heating rate of 10°C/min in an air atmosphere. The measurements were performed on cylindrical samples. Elementary analyses were performed by the Centre National de la Recherche Scientifique (CNRS) Service Central d'Analyse, Solaize, France.

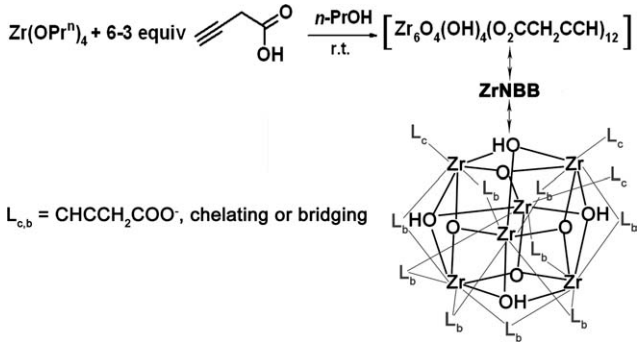

Figure 1 Synthesis of the ZrNBB and hypothesized structure scheme of the cluster formula $[Zr_6O_4(OH)_4(O_2CCH_2CCH)_{12}]$.

RESULTS AND DISCUSSION

The ZrNBB was synthesized by the addition of 70% $Zr(OPr^n)_4$ in *n*-propanol to 3-butynoic acid. The mixture was stirred for 1 h and washed then with *n*-propanol to remove the excess organic ligand. The reaction outcome did not change when the order of the reaction components was inverted with 6 or 3 equiv of 3-butynoic acid or with a concentration range of the alkyne from 5 to 14*M*. The product, obtained as a white solid, was analyzed via FTIR spectroscopy, NMR, energy-dispersive X-ray analysis, DSC, thermogravimetric analysis, and elementary analysis (C, 28.61 wt %; H, 2.76 wt %; and Zr, 30.51 wt %). The data were consistent with the cluster formula $Zr_6O_4(OH)_4(O_2CCH_2C{\equiv}CH)_{12}$ (Fig. 1). Energy-dispersive X-ray analysis measurements [Fig. 2(A,B)] established the homogeneity and constant composition of the sample without any significant chemical alteration. Characterization of the solid by single-crystal or X-ray diffraction was not possible because of the low crystallinity of the material.

The FTIR spectrum of the synthesized ZrNBB complex, reported in Figure 3(B), shows the $\nu_{\equiv C-H}$ and $\nu_{C\equiv C}$ stretching bands of the monosubstituted alkyne at 3286 and 2109 cm^{-1}. The band associated with the C≡C bond was lowered by approximately 18 cm^{-1} compared to the same band in the free 3-butynoic acid [Fig. 3(A)]. The shift of the C≡C stretching vibration was too small to indicate a proper σ or π interaction between the alkyne and the zirconium. In fact, for a pure σ interaction, the C≡C stretching vibration appeared about 100 cm^{-1} lower than that for the corresponding free alkyne. In the case of pure π interaction, the C≡C frequency is lower by approximately 230–130 cm^{-1}.[5] The $\nu_{C=O}$ stretching vibration band of the free 3-butynoic acid ligand, observed in the 1727–1690-cm^{-1} region, also disappeared, splitting at lower frequencies into the absorption bands of the carboxylate group (ν^-_{CO2} asymmetric stretching vibration at 1560 cm^{-1} and ν^-_{CO2} symmetric stretching vibration at 1429 and 1387 cm^{-1}). Their values and relative positions [wavenumber difference ($\Delta\nu$) ≈ 131 cm^{-1} and $\Delta\nu \approx 173$ cm^{-1}, where $\Delta\nu_{CO2Na} = 211$ cm^{-1} (1587 and 1376 cm^{-1})] suggested a chelating and bridging

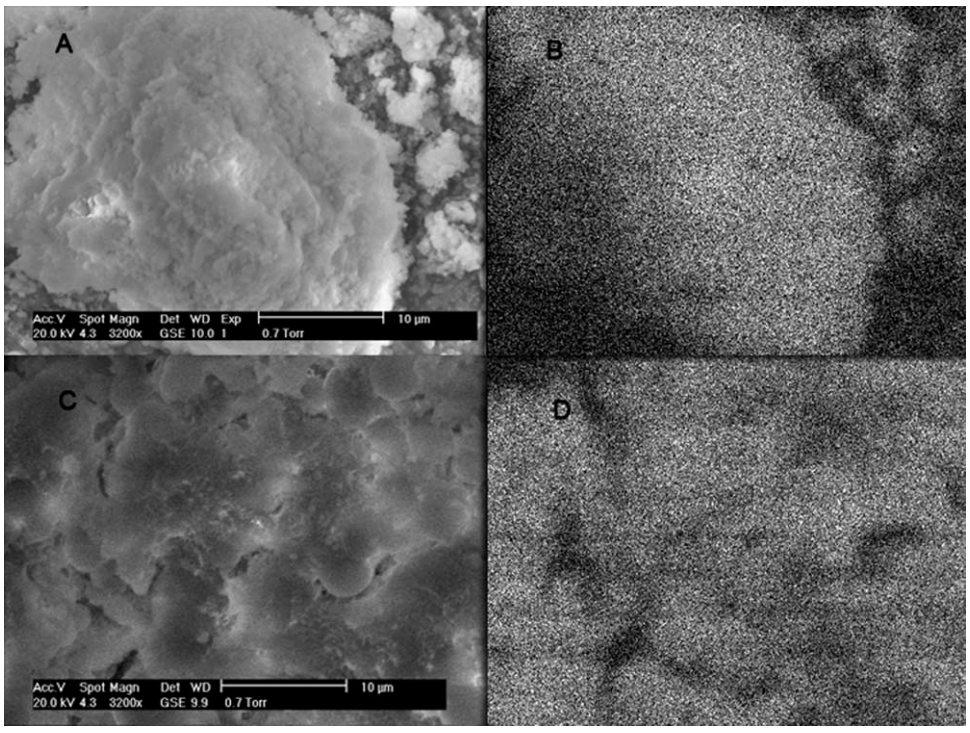

Figure 2 (A,B) ESEM images of ZrNBB obtained after 1 h stirring and relative EDAX mapping of zirconium and (C,D) ESEM images of ZrNBB obtained after 3 days of stirring and relative EDAX mapping of zirconium.

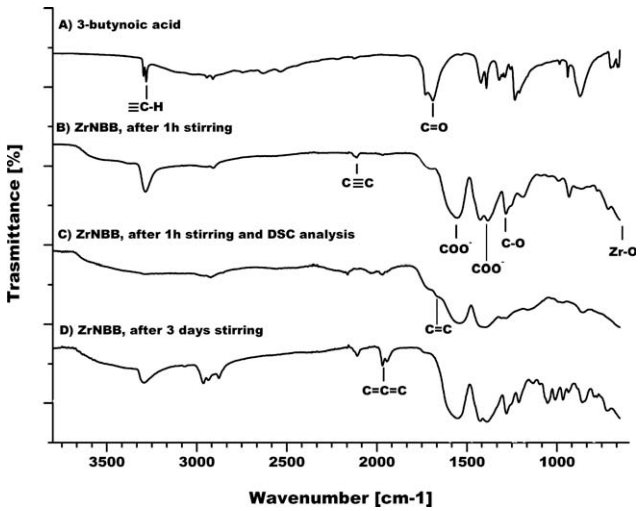

Figure 3 FTIR spectra of (A) 3-butynoic acid and (B) ZrNBB obtained with a reaction time of 1 h, (C) ZrNBB obtained with a reaction time of 1 h and after DSC analysis, and (D) ZrNBB obtained with a reaction time of 3 days.

coordination mode of the carboxylate ligand to the zirconium.[6] The existence in the ZrNBB complex of a small percentage of the organic ligand in its buta-2,3-dienoate form was shown by the $\nu_{C=C=C}$ asymmetric stretching vibration of this monosubstituted allene. The band was composed of two peaks at 1968 and 1945 cm^{-1} because of the presence of the strong polar substituent carboxylate.

In the ^{13}C-MAS analysis [Fig. 4(B)], the set of signals of the 3-butynoate (alkynic) and buta-2,3-dienoate (allenic) isomers could be clearly assigned. Moreover, a convolution analysis of the carboxylate peak showed a decomposition of the signal into three different components, which could be correlated to three inequivalent carboxylate carbons. On

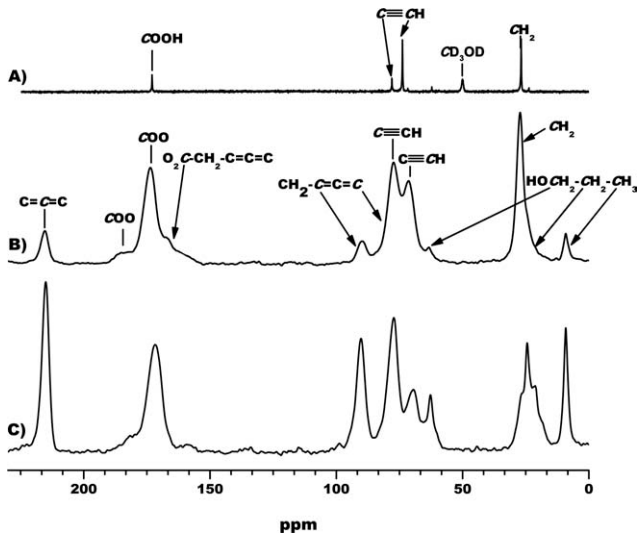

Figure 4 ^{13}C-MAS spectra of (A) 3-butynoic acid in CD_3OD and (B) ZrNBB after 1 h stirring and (C) ZrNBB after 3 days of stirring.

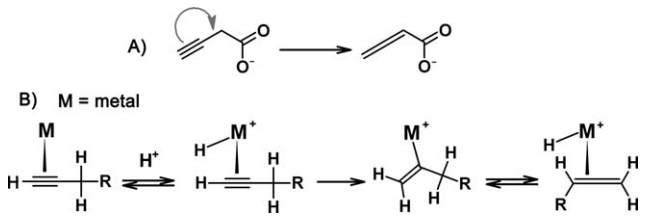

Figure 5 (A) Isomerization of 3-butynoate to buta-2,3-dienoate and (B) simplified isomerization mechanism of alkyne to allene induced by a metal such as rhodium and rhenium in an acidic environment.

the basis of previous carboxylate–metal complex studies[7] and, in particular, the studies performed by Schubert and coworkers[8] on zirconium clusters, these three signals were tentatively assigned to a chelating carboxylate ligand position (184.2 ppm) and two nonequivalent bridging carboxylate ligand positions (173.6 and 167.1 ppm). ^1H-NMR analysis performed in acetone–d^6 also showed partial overlapped broad and unresolved signals of inequivalent 3-butynoate ligands (the broadness was attributed to their mutual exchange)[9] and well-defined signals of the buta-2,3-dienoate isomer (5.60 triplet and 5.27 doublet ppm). The impossibility of observing a two-dimensional NMR correlation between the broad and unstructured peaks prevented the determination of a definitive structure and symmetry for the zirconium complex. A similar dynamic situation was observed in DMSO–d^6, where the mutual carboxylate ligand exchange was accompanied by fast isomerization of the alkyne to the allene. Probably, the low crystallinity of the complex was due to this isomerization phenomenon, which prevented the obtainment of a well-defined structure [Fig. 5(A)]. Interestingly, no isomerization was observed for the sole 3-butynoic acid ligand in DMSO–d^6 or other NMR solvents.

The DSC curve of the ZrNBB [Fig. 6(A)] showed an exothermic event with an initial reaction temperature of 117°C and the maximum of the peak at 154°C, followed by a shoulder. The change in enthalpy was 260 J/g, with a sample mass loss of 8%. The event was not reversible, and after performing a second DSC analysis [Fig. 6(B)] on the same sample, we observed only a small exothermic event (17 J/g, maximum temperature (T_{max}) = 110°C) with a mass loss of 1%. The infrared spectrum of the sample recovered after DSC [Fig. 3(C)] did not show anymore the absorption bands of the alkyne, the $\nu_{C=C=C}$ band of the allene was almost absent, and a new shoulder, assigned to the $\nu_{C=C}$ stretching vibration of a nonconjugate double bond, appeared at 1664 cm^{-1}. This was in accordance with the polymerization of ZrNBB proceeding by isomerization of the alkyne to the allene. In the DSC analysis of the ZrNBB sample doped with 3 wt % BPO [Fig. 6(E)], the thermal radical initiator accelerated the first polymerization event and shifted T_{max} to 135°C.

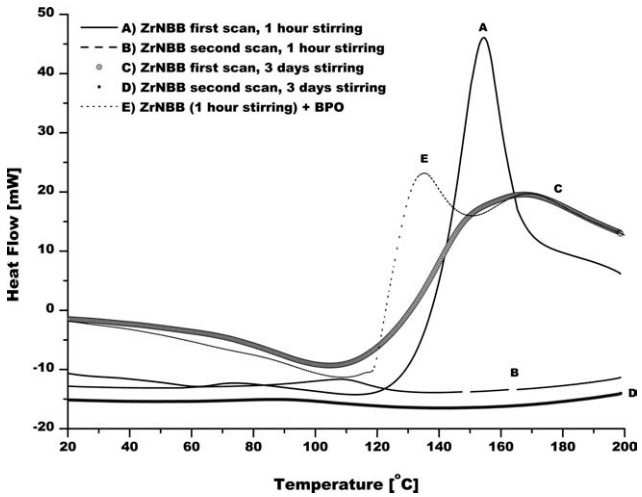

Figure 6 DSC curve of the ZrNBB sample. The analysis was performed from 30 to 200°C in nitrogen with a heating rate of 10°C/min. The sample of curve E was composed of ZrNBB obtained with a reaction time of 1 h and 3 wt % BPO.

A longer reaction time was observed to vary the outcome of the synthesis. Leaving the $Zr(OPr^n)_4$ and 3-butynoic acid mixture stirring for more than 1 day (or alternatively letting the solutions of the two components slowly diffuse into each other) evidently favored the isomerization of the 3-butynoate to the buta-2,3-dienoate. The recovered product [Fig. 2(C,D)], characterized by a light orange color, presented an elementary composition as follows: C, 30.35 wt %; H, 3.60 wt %; and Zr, 29.64 wt %; this is still in accordance with $Zr_6O_4(OH)_4(O_2CCH_2C{\equiv}CH)_{12}$ but; this is still in accordance with $Zr_6O_4(OH)_4(O_2CCH_2CCH_2)_{12}$ but the solid in this case was soluble only in high polar solvents such as DMSO and DMF was soluble only in high-polar solvents such as DMSO and DMF. The FTIR [Fig. 3(D)] and ^{13}C-MAS [Fig. 4(C)] spectra confirmed a higher degree of isomerization of the 3-butynoate to the buta-2,3-dienoate without further changes in the structure of the complex.

The DSC analysis [Fig. 6(C)] showed a single polymerization event with an initial reaction temperature of 106°C and the maximum of the peak at 174°C, with an associated enthalpy change of 149 J/g and a sample mass loss of 14%. The higher percentage of solvent trapped in the sample (detected also by ^{13}C-MAS) was considered responsible for the higher mass loss, whereas the lower enthalpy change could be explained by the higher percentage of the buta-2,3-dienoate ligand in the ZrNBB sample. A second DSC cycle [Fig. 6(D)] no longer showed the exothermic event and had a mass loss of 0.4%. In the FTIR spectrum of the sample recovered after the DSC, only the shoulder of the $\nu_{C=C}$ stretching vibration was present.

Base catalysts such as *t*-BuOK are known to be quite effective for the preparation of allenes from the corresponding propargyl derivatives.[10] Thus, in our case, the *n*-propoxide molecules derived from $Zr(OPr^n)_4$ could have been responsible for the observed isomerization of the carboxylate ligand. However, the synthesis of the ZrNBB complex was performed in an acidic environment (6 equiv of carboxylic acid), and a fast isomerization was also observed for the purified ZrNBB complex in DMSO–d^6 in the absence of $Zr(OPr^n)_4$. Because isomerization of alkyne to allene have been reported for alkyne complexes of rhodium,[11] manganese,[12] and rhenium,[13] where it was the metal itself that promoted the isomerization, a mechanism of this type could be also considered [Fig. 5(B)].

In general, radical polymerization of allene derivatives are reported to also take place in the absence of a radical initiator upon heating of the monomers.[14] The initiating species, which arises from a dimerization process, selectively attacks the center carbon of the allene monomer to produce a stable allyl radical as an intermediate; this leads to a polymer with external double bonds.[15] Contrarily, propargyl derivatives have poor radical polymerizability and high chain-transfer constants. Therefore, the polymerization follows the isomerization of the alkyne into allene derivatives.

The viscoelastic proprieties of a bulk sample obtained from $Zr(OPr^n)_4$ and 3-butynoic acid after 1 day of stirring in the absence of a radical initiator were analyzed via DMS in compression mode (Fig. 7). The specimen obtained from the reaction was monolithic yet fragile. The analysis of the sample in the temperature range 30–300°C showed an important increase in E' around 150°C initial storage modulus (E'_{initial}) = 6.98×10^7 and final storage modulus (E'_{final}) = 8.91×10^8) and a second but smaller

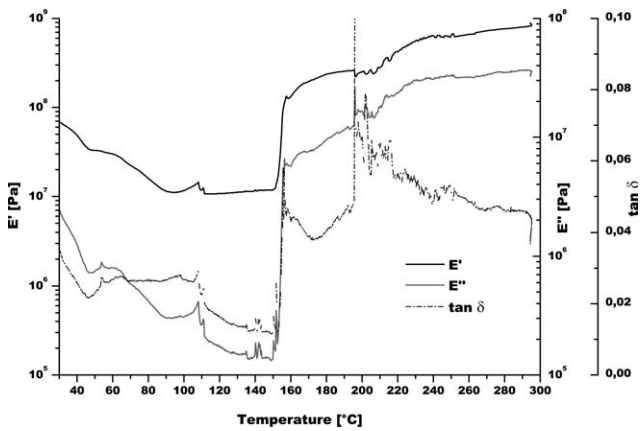

Figure 7 First DMS run of the ZrNBB sample performed in compression mode (oscillation frequency = 1 Hz, force = 100 mN) from 30 to 300°C at a heating rate of 2°C/min.

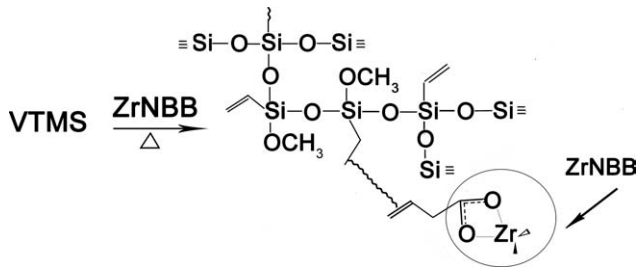

Figure 8 Synthesis of the copolymers of ZrNBB and VTMS prepared both with and without BPO. A schematic example of the type of bonds formed in the copolymers is shown.

increase around 200°C, which then followed a constant slight raise until 300°C. The first increase of E' agreed with a polymerization phenomena, and the second agreed with the establishment of a higher crosslink density. The low value of tan δ (<0.1 in the observed temperature range) indicated a reduced molecular mobility in the material. The similar trend of storage modulus (E') and loss modulus (E'') curves confirmed that the material was homogeneously stiff and far away from any glass-transition point. Hence, it was no surprise that the recovered bulk sample was integral with a smooth surface, showing only slight shrinkage. In the a second run, a slight improvement of E' was observed ($E'_{\text{initial}} = 6.47 \times 10^8$ and $E'_{\text{final}} = 9.097 \times 10^8$).

The copolymers of ZrNBB and VTMS were prepared both with and without BPO as a radical initiator (Zr/Si molar ratio = 1 : 40; Fig. 8).[3(a,b),16] FTIR analyses [Fig. 9(A,B)] of both copolymers had the characteristic $\nu_{C=C}$ band (1602 cm^{-1}) of the vinyl group attached to the siloxane chain with the $\nu_{Si-O-Si}$ (1078 cm^{-1}) band, along with the $\nu_{C=C=C}$ (1971 and 1944 cm^{-1}) and ν^{-}_{CO2} (1562 and 1433 cm^{-1}) bands of ZrNBB. Both hybrid materials showed

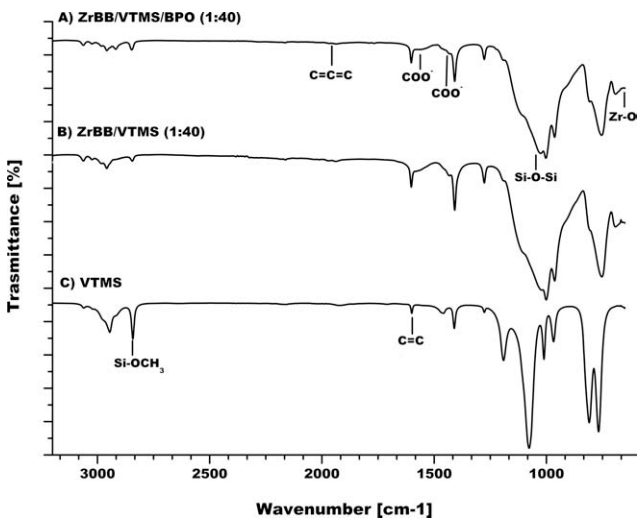

Figure 9 FTIR spectra of (A) ZrNBB/VTMS/BPO with a zirconium-to-silicium ratio of 1 : 40, (B) ZrNBB/VTMS with a zirconium-to-silicium ratio of 1 : 40, and (C) VTMS.

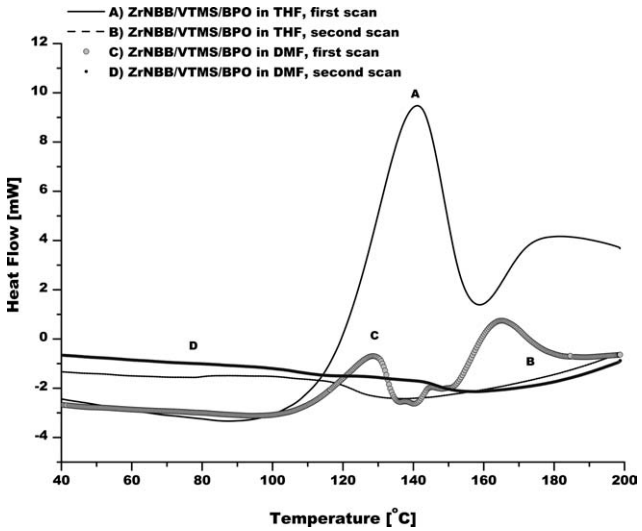

Figure 10 DSC curves of the xerogels (A) ZrNBB/VTMS/BPO synthesized in THF, first scan; (B) ZrNBB/VTMS/BPO synthesized in THF, second scan; (C) ZrNBB/VTMS/BPO synthesized in DMF, first scan; and (D) ZrNBB/VTMS/BPO synthesized in DMF, second scan. The analyses were performed from 30 to 200°C in nitrogen with a heating rate of 10°C/min.

transparency, which was gradually lost during thermal aging. In the DSC curve [Fig. 10(A)], a main exothermal polymerization peak (T_{max} = 141°C) and a high-temperature shoulder, attributed to the polymerization of steric hindered multiple bonds of the zirconium oxocluster, were visible. The polymerization heat, calculated including the shoulder, was 51 J/g, and the mass loss was −7%.

The same polymerization event was also visible in the DMS curves of the copolymers (Figs. 11 and 12). For the hybrid material synthesized without BPO, the polymerization was spread over a wider temperature range. After this event, G' of the specimens increased constantly. In the shear mode analysis, the G' curve

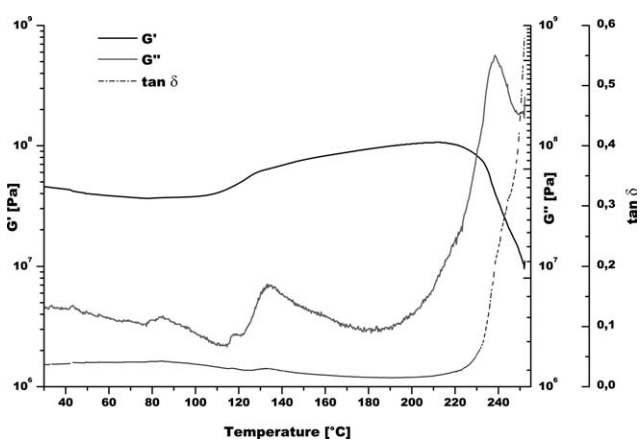

Figure 11 First DMS run of the ZrNBB/VTMS/BPO sample performed in shear mode (oscillation frequency = 1 Hz, force = 1000 mN) from 30 to 300°C at a heating rate of 2°C min^{-1}.

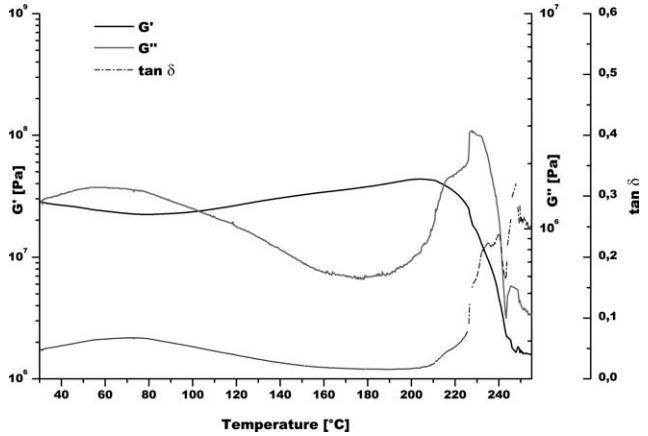

Figure 12 First DMS run of the ZrNBB/VTMS sample performed in shear mode (oscillation frequency = 1 Hz, force = 1000 mN) from 30 to 300°C at a heating rate of 2°C min^{-1}.

ended with a sharp drop corresponding to the glass-transition temperature ($T_{gG''}$ = 238°C with BPO and $T_{gG''}$ = 227°C without). The copolymer synthesized without BPO presented a slightly lower glass-transition temperature (T_g), which could have been associated with a lower average molecular mass. A higher free volume related to a lower molecular mass could also explain the higher volume contraction of this sample (−11 and −10% for the first and second runs, respectively) compared to the sample obtained with BPO (−5 and −3% for the first and second runs, respectively). In the second DMS runs, not reported here, the copolymer synthesized with BPO showed an increased G' from 1.18×10^7 to 7.25×10^7 Pa, but no $T_{gG''}$ was observed up to 300°C. The copolymer synthesized without BPO presented a higher $T_{gG''}$ value (244°C) compared to the first run.

When a polar solvent such as DMF was employed in the preparation of the ZrNBB/VTMS/BPO copolymer, different thermomechanical behavior of the material was observed. The DSC analysis [Fig. 10(C,D)] showed two major exothermic events characterized by T_{max} values of 129 and 165°C, with a total enthalpy change of 18 J/g and a mass loss of −6%. DMS analysis (Fig. 13) showed a relaxation phenomena around 110°C, after which the value of G' increased to 6.40×10^7 Pa (reached at 152°C) and then decreased to arrive at a $T_{gG''}$ of 211°C. The presence of the DMF peaks in the ^{13}C-MAS spectrum of the ZrNBB/VTMS/BPO copolymer suggested possible participation of the solvent in a ligand-exchange process.

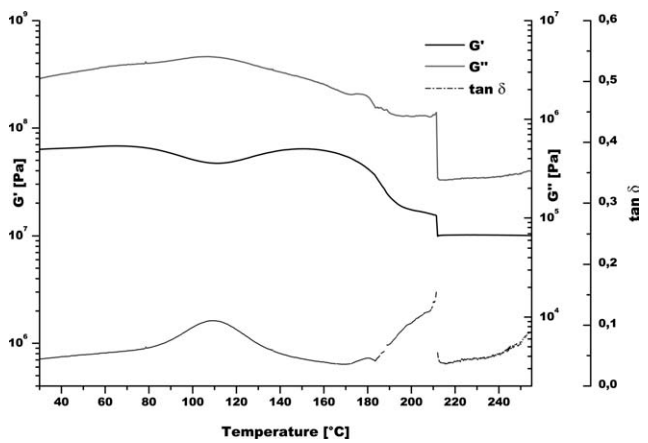

Figure 13 First DMS run of the ZrNBB/VTMS sample prepared in DMF performed in shear mode (oscillation frequency = 1 Hz, force = 1000 mN) from 30 to 300°C at a heating rate of 2°C min^{-1}.

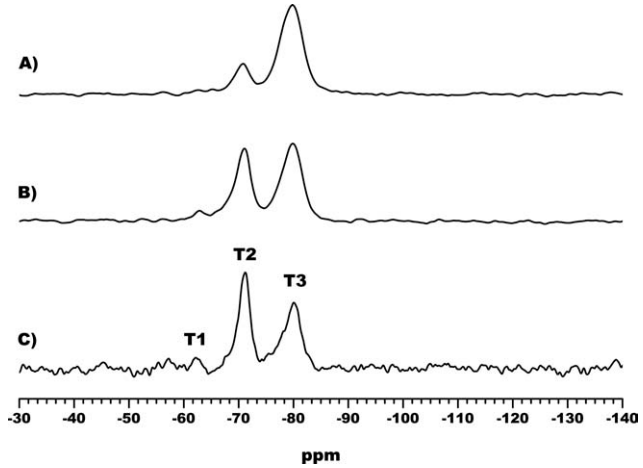

Figure 14 ^{29}Si-MAS of (A) ZrNBB/VTMS/BPO (1 : 40) synthesized in DMF, (B) ZrNBB/VTMS (1 : 40) synthesized in THF, and (C) ZrNBB/VTMS/BPO (1 : 40) synthesized in THF.

The ^{29}Si-MAS spectra of the copolymers synthesized with THF or DMF as a solvent, with or without BPO, are reported in Figure 14. When THF was employed with BPO [Fig. 14(C)], T1 (3.7%), T2 (48.8%), and T3 (47.4%), or without [Fig. 14(B)], T1 (11.7%), T2 (38.5%), and T3 (49.7%), the T2 [$ROSi(OSi)_2R'$] and T3 [$Si(OSi)_3R'$] units were the main species. When DMF instead of THF was employed [Fig. 14(A)], the T3 (74,1%) units [$Si(OSi)_3R'$] became predominant (T1 = 3.1% and T2 = 22.8%).

CONCLUSIONS

In conclusion, a new ZrNBB was synthesized with the 3-butynoic acid ligand. The 3-butynoate involved in the ZrNBB was observed to undergo isomerization to buta-2,3-dienoate when the sample was heated or left in solution for a long time (short times in the case of highly polar solvents). The isomerization of the 3-butynoate to buta-2,3-dienoate was also observed to trigger the polymerization process. When a monolithic ZrNBB sample was exposed to a sinusoidal stress in the temperature range 30–300°C, the strain of the material was observed to drastically improve around 150°C; we measured in the first run

of DMS analysis a final G' of 8.91×10^8 Pa. Hybrid inorganic–organic materials were prepared by the radical copolymerization of ZrNBB and VTMS, both with and without BPO. The copolymers showed interesting thermomechanical proprieties and a high T_g (238°C), together with a small mass loss and solid shrinkage. The ^{29}Si-MAS spectra of the copolymers synthesized in THF indicated as a main species the T2 [$ROSi(OSi)_2R'$] and T3 [$Si(OSi)_3R'$] units. It is worth noticing that the prepared hybrid materials were obtained with only a low ratio of the ZrNBB component (Zr/Si molar ratio = 1 : 40); this leaves space for further improvement. More in-depth studies need to be performed to better characterize the ZrNBB and understand the spontaneous 3-butynoate ligand isomerization and polymerization processes.

The authors thank Dr. Emanuela Callone and Prof. Graziano Guella for the solid- and liquid-state NMR measurements. The authors also thank Prof. Luca Fambri for the helpful discussion.

References

1. Schubert, U. Chem Soc Rev 2011, 40, 575.
2. (a) Schubert, U. Chem Mater 2001, 13, 3487; (b) Schubert, U. Macromol Symp 2008, 267, 1; (c) Schubert, U. J Sol–Gel Sci Technol 2004, 31, 19; (d) Faccini, F.; Fric, H.; Schubert, U.; Wendel, E.; Tsetsgee, O.; Müller, K.; Bertagnolli, H.; Venzoa, A.; Gross, S. J Mater Chem 2007, 17, 3297.
3. (a) Di Maggio, R.; Dirè, S.; Callone, E.; Girardi, F.; Kickelbick, G. Polymer 2010, 51, 832; (b) Di Maggio, R.; Dirè, S.; Callone, E.; Girardi, F.; Kickelbick, G. J Sol–Gel Sci Technol 2008, 48, 168; (c) Girardi, F.; Cappello, E.; Della Volpe, C.; Negri, M.; Müeller, K.; Di Maggio, R. J Sol–Gel Sci Technol, to appear.
4. Heinz, P.; Puchberger, M.; Bendova, M.; Baumann, S. O.; Schubert, U. Dalton Trans 2010, 39, 7640.
5. Socrates, G. Infrared and Raman Characteristic Group Frequencies; Wiley: Hoboken, NJ, 2006.
6. (a) Deacon, G. B.; Phillips, R. J. Coord Chem Rev 1980, 33, 227; (b) Papageorgiou, S. K.; Kouvelos, E. P.; Favvas, E. P.; Sapalidis, A. A.; Romanos, G. E.; Katsaros, F. K. Carbohydr Res 2010, 345, 469; (c) Doeuff, S.; Henry, M.; Sanchez, C.; Livage, J. J Non-Cryst Solids 1987, 8, 206; (d) Barboux-Doeuff, S.; Sanchez, C. Mater Res Bull 1994, 29, 1; (e) Perrin, F. X.; Nguyen, V.; Vernet, J. L. J Sol–Gel Sci Technol 2003, 28, 205; (f) Faccini, F.; Fric, H.; Schubert, U.; Wendel, E.; Tsetsgee, O.; Müller, K.; Bertagnolli, H.; Venzo, A.; Gross, S. J Mater Chem 2007, 17, 3297.
7. Ye, B.-H.; Li, X.-Y.; Williams, I. D.; Chen, X.-M. Inorg Chem 2002, 41, 6426.
8. (a) Kogler, F. R.; Jupa, M.; Puchberger, M.; Schubert, U. J Mater Chem 2004, 14, 3133; (b) Puchberger, M.; Kogler, F. R.; Jupa, M.; Gross, S.; Fric, H.; Kickelbick, G.; Schubert, U. Eur J Inorg Chem 2006, 94, 3283.
9. Walther, P.; Puchberger, M.; Kogler, F. R.; Schwarz, K.; Schubert, U. Phys Chem Chem Phys 2009, 11, 3640.
10. (a) Tomita, I.; Yamamura, I.; Endo, T. J Polym Sci Part A: Polym Chem 1996, 34, 1853; (b) Tomita, I.; Yamamura, I.; Endo, T. Polym Prepr Jpn 1993, 42, 1856.
11. Wolf, J.; Werner, H. Organometallics 1987, 6, 1164.
12. (a) Franck-Neumann, M.; Brion, F. Angew Chem Int Ed Engl 1979, 18, 688; (b) Coughlan, S. M.; Yang, G. K. J Organomet Chem 1993, 450, 151.
13. Casey, C. P.; Brady, J. T. Organometallics 1998, 17, 4620.
14. Endo, T.; Tomita, I. Prog Polym Sci 1997, 22, 565.
15. Yokozawa, T.; Tanaka, M.; Endo, T. Chem Lett 1987, 1831.
16. Kickelbick, G. J Sol–Gel Sci Technol 2008, 46, 281.